MOLECULAR MODELS:

PHYSICAL

- FRAMEWORK
- SPACE FILLING

MATHEMATICAL

- QUANTUM MECHANICS
- CLASSICAL (EMPIRICAL) POTENTIAL FUNCTIONS
- STATISTICAL OR DATABASE DERIVED

History of Computer-Based Molecular Models

Physical Organic Chemistry

Westheimer–Hendrickson–Wiberg

Lifson

Biophysics & Biochemistry

Ramachandran

Scheraga

Amber, CHARMM, Gromos, Discover, etc.

DIPOLE MOMENT OF CARBON MONOXIDE

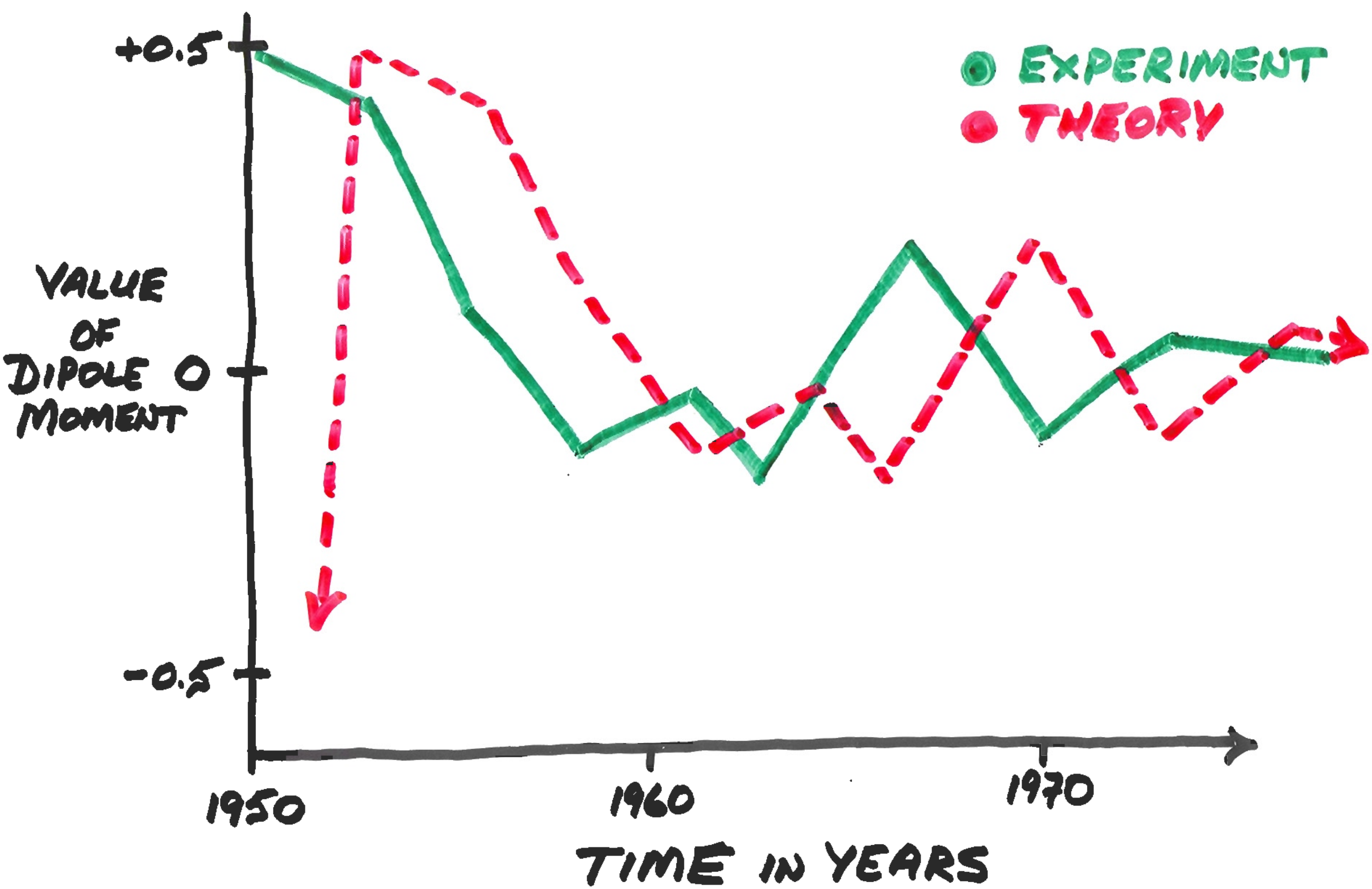

USES OF POTENTIAL ENERGY FUNCTIONS:

1. ENERGY MINIMIZATION
2. MOLECULAR DYNAMICS
3. MONTE CARLO SIMULATIONS
4. VIBRATIONAL ANALYSIS
5. X-RAY REFINEMENT
6. CONSTRAINT / RESTRAINT MODELING (NOE's etc.)
7. FREE ENERGY DIFFERENCES

PARTIAL LIST OF MOLECULAR MECHANICS SOFTWARE PACKAGES

AMBER	Peter Kollman, Univ. of California, San Francisco
ARGOS	J. Andrew McCammon, Univ. of California, San Diego
BOSS	William Jorgensen, Yale University
BOYD	Richard Boyd, University of Utah
BRUGEL	Shoshona Wodak, Free University of Brussels
CEDAR	Jan Hermans, University of North Carolina
CFF	Shneior Lifson, Weizmann Institute
CHARMM	Martin Karplus, Harvard University
CHARMM/GEMM	Bernard Brooks, National Institutes of Health, Bethesda
DELPHI	Bastian van de Graaf, Delft University of Technology
DISCOVER	Arne Hagler, BIOSYM Technologies/Molecular Simulations
ECEPP	Harold Scheraga, Cornell University
ENCAD	Michael Levitt, Stanford University
FANTOM	Werner Braun, University of Texas, Galveston
FEDER/2	Nobuhiro Go, Kyoto University
GROMACS	Herman Berendsen, University of Groningen
GROMOS	Wilfred van Gunsteren, BIOMOS and ETH, Zurich
IMPACT	Ronald Levy, Rutgers University
MACROMODEL	W. Clark Still, Columbia University
MM2/MM3/MM4	N. Lou Allinger, University of Georgia
MMC	Cliff Dykstra, Indiana Univ.–Purdue Univ. at Indianapolis
MMFF	Tom Halgren, Merck Research Laboratories, Rahway
MOIL	Ron Elber, The Hebrew University, Jerusalem
MOLARIS	Arieh Warshal, University of Southern California
MOLDY	Keith Refson, Oxford University
ORAL	Karel Zimmerman, INRA, Jouy-en-Josas, France
ORIENT	Anthony Stone, Cambridge University
PEFF	Jan Dillen, University of Pretoria, South Africa
SPASMS	David Spellmeyer and the Kollman Group, UCSF
TINKER	Jay Ponder, Washington University, St. Louis
XPLOR	Axel Brunger, Yale University
YAMMP	Stephen Harvey, University of Alabama, Birmingham
YETI	Angelo Vedani, University of Kansas

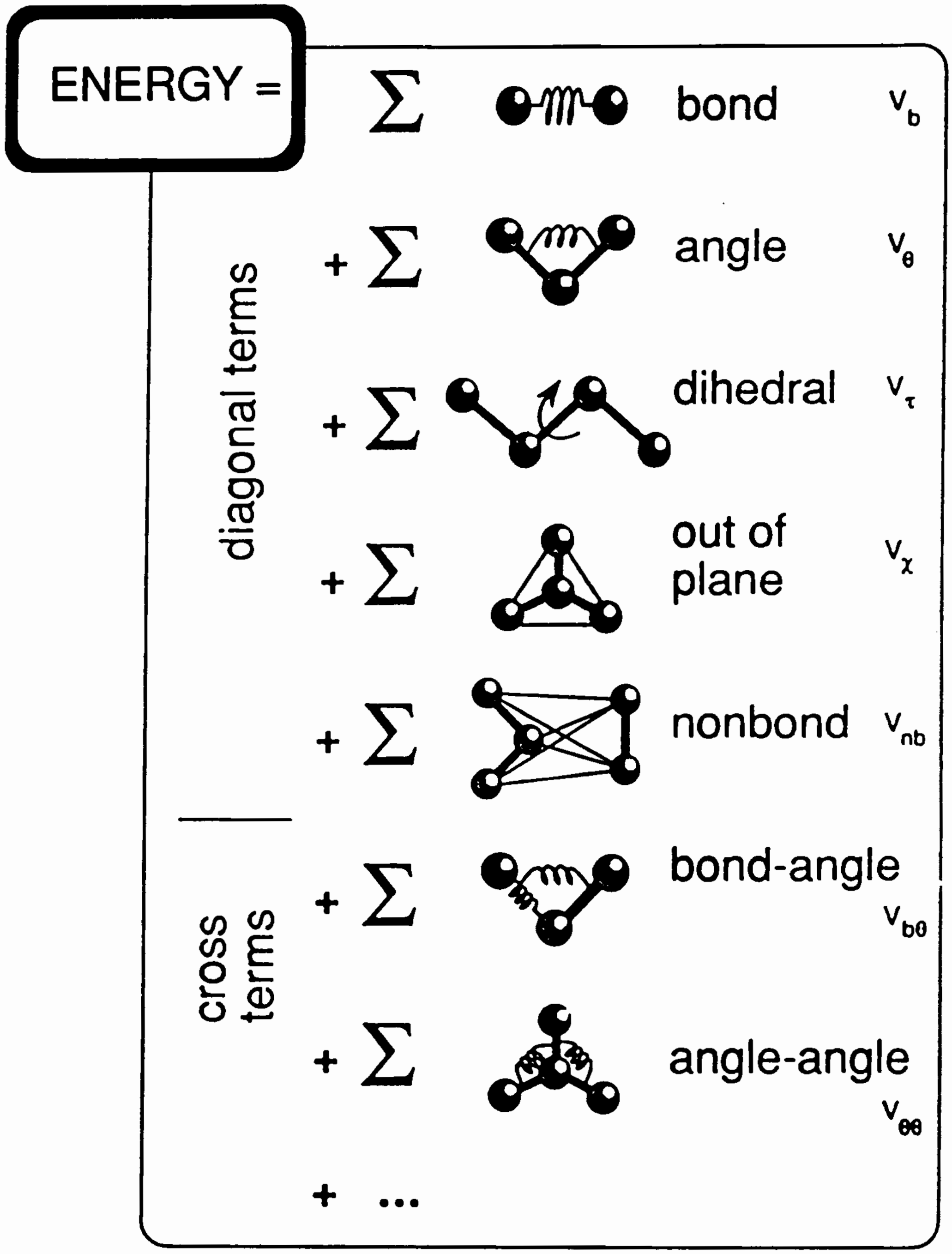

Figure 1 Schematic of molecular force field expression. Diagonal terms refer to interactions that can be expressed as a function of a single internal coordinate, whereas cross terms introduce coupled interactions involving two or more coordinates.

"STERIC" ENERGY

$$E_{STERIC} = E_{BOND} + E_{ANGLE}$$
$$+ E_{STR/BEND} + E_{TORSION}$$
$$+ E_{VDW} + E_{CHG-CHG}$$
$$+ E_{CHG-DPL} + E_{DPL-DPL} + E_{HBOND}$$
$$+ E_{SOLVENT} + \ldots$$

$$E_{STERIC} \xrightarrow[\text{INCREMENT METHOD}]{\text{BOND}} \Delta H_f^\circ$$

ACCURACY –

HYDROCARBONS	0.42 KCAL
ETHERS	0.50 KCAL
BIOPOLYMERS	???

Table 1 MM3 Heat of Formation Data for Aliphatic Amines (kcal/mol)[a]

$H_f°$ calc	$H_f°$ exp	Difference (calc − exp)	Compound
−5.04	−5.50	0.46	Methylamine
−4.04	−4.43	0.39	Dimethylamine
−6.09	−5.67	−0.42	Trimethylamine
−11.92	−11.35	−0.57	Ethylamine
−17.41	−17.33	−0.08	Diethylamine
−21.49	−22.17	0.68	Triethylamine
−16.95	−16.77	−0.18	*n*-Propylamine
−20.31	−20.02	−0.29	Isopropylamine
−21.85	−21.98	0.13	*n*-Butylamine
−24.31	−25.06	0.75	*sec*-Butylamine
−23.51	−23.57	0.06	Isobutylamine
−28.90	−28.90	0.00	*tert*-Butylamine
−11.83	−11.76	−0.07	Piperidine
−20.30	−20.19	−0.11	2-Methylpiperidine
9.90	9.90	0.00	Cyclobutylamine
−13.70	−13.13	−0.57	Cyclopentylamine
−1.29	−1.03	−0.26	Quinuclidine
−31.67	−34.41	2.74	Diisopropylamine
−24.86	−2.06	0.20	Cyclohexylamine
−0.94	−0.80	−0.14	Pyrrolidine
24.62	24.62	0.00	Azetane

[a]Best values: C−N = 6.173, N−H = −1.178, N−Me = 2.965, NISO = −4.442, NSEC = 2.635, TBUN = −8.867, NCBU = 1.171, 8-56 = 2.617. Fixed values: NTER = 0.000. Standard deviation = 0.354. See ref. 44 for definitions.

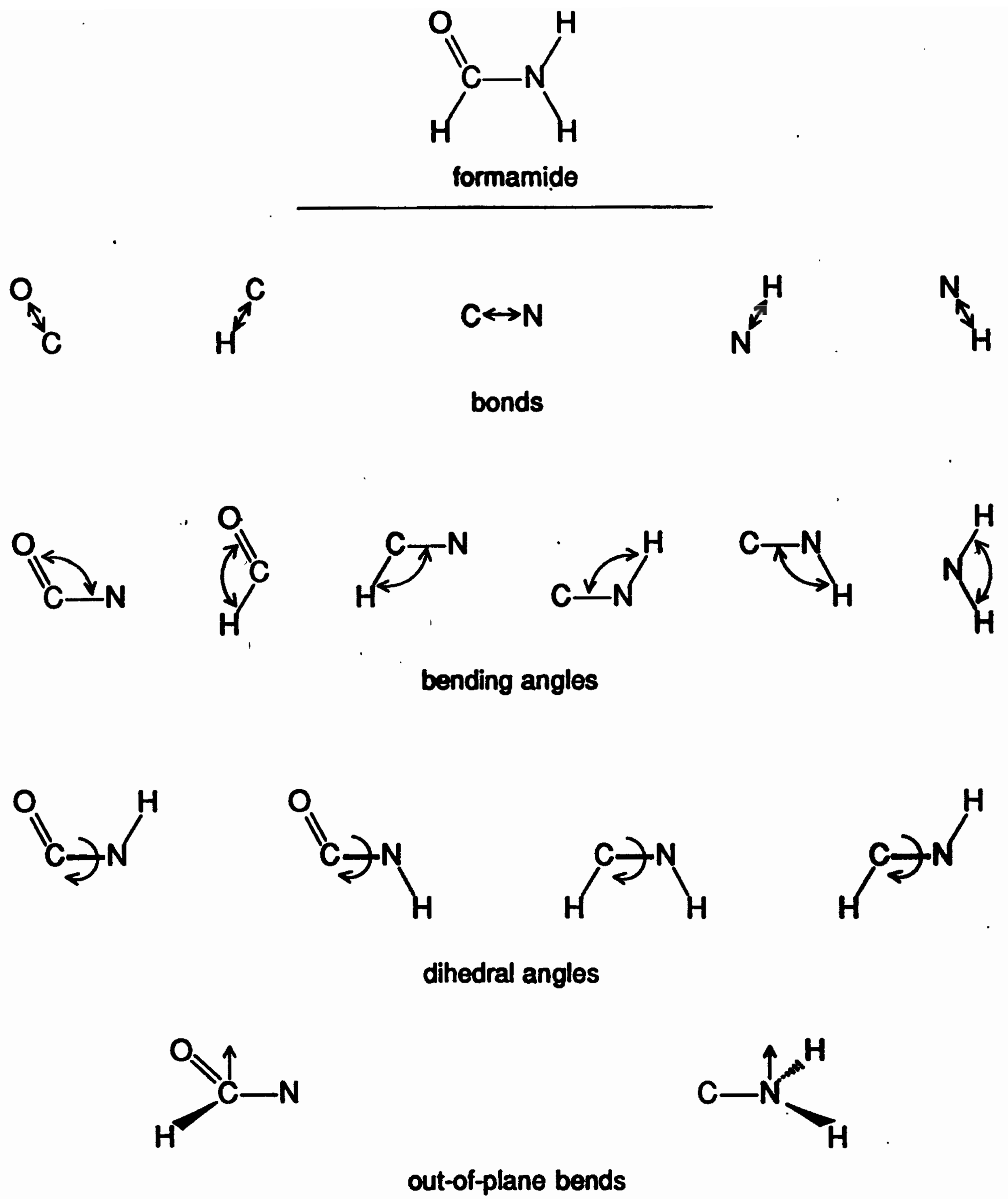

Figure 2 Valence coordinates in formamide. The 12 nonredundant coordinates of formamide [$3n - 6 = (3 \times 6) - 6 = 12$] can be represented by up to 17 valence coordinates. The extra 5 coordinates introduce redundancies that must be treated carefully in order to fit transferable parameters.

BOND POTENTIAL

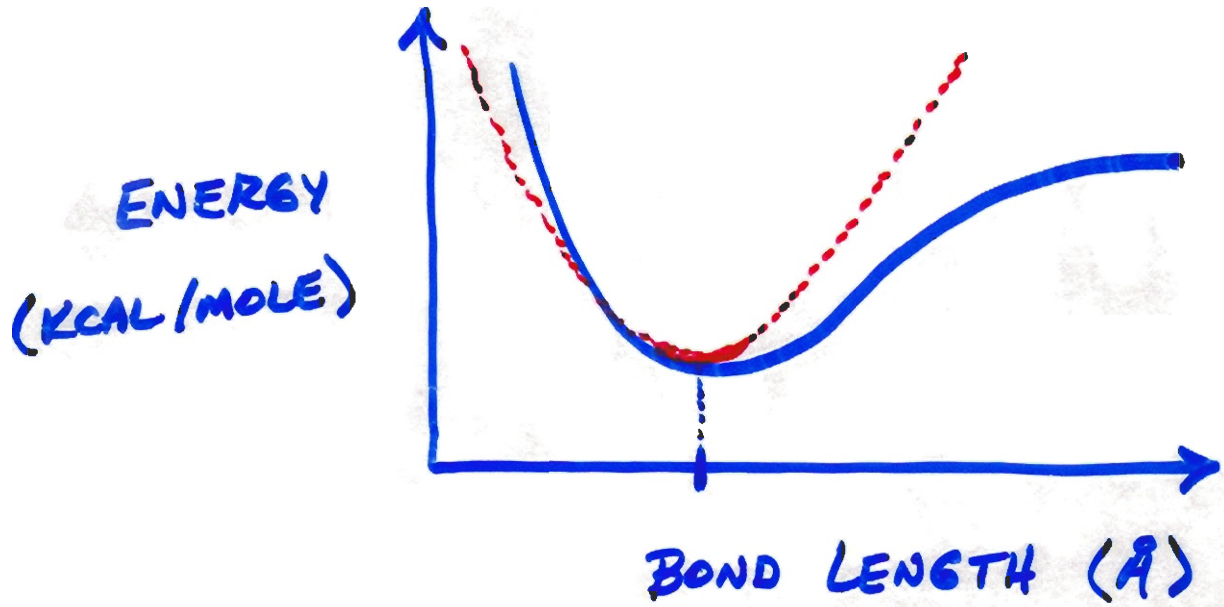

MORSE: $E(R) = D_E \cdot \{1 - e^{-\alpha(R-R_0)}\}^2$

D_E = DISSOCIATION ENERGY

$\alpha = \sqrt{k/2D_E} \approx 2\,Å^{-1}$

HARMONIC: $E(R) = \frac{1}{2} k\,(R-R_0)^2$

QUESTION: WHERE DO WE GET VALUES FOR k <u>AND</u> R_0?

Table 1 Transferability of *ab Initio* Bond Parameters in Alkanes[117,121]

Molecule	Bond length (Å)	Force constant (k_{ch})	Bond length (b_{cc})	Force constant (k_{cc})
Ethane	1.086	5.800	1.527	5.109
Propane	1.086	5.769	1.528	4.962
	1.087	5.690	—	—
	1.086	5.803	—	—
Butane	1.086	5.801	1.528	4.960
	1.086	5.769	—	—
	1.088	5.659	1.530	4.910
Pentane	1.086	5.799	—	—
	1.086	5.770	—	—
	1.088	5.662	—	—
	1.089	5.628	—	—
Cyclopropane	1.076	6.161	1.497	5.125
Cyclobutane[a]	1.084	5.813	1.549	4.669
Cyclobutane[b]	1.084	5.829	1.545	4.617
	1.085	5.790	—	—
Cyclopentane	1.085	5.799	1.531	4.875
	1.085	5.773	—	—
	1.085	5.797	—	—
	1.088	5.670	—	—
	1.086	5.710	—	—

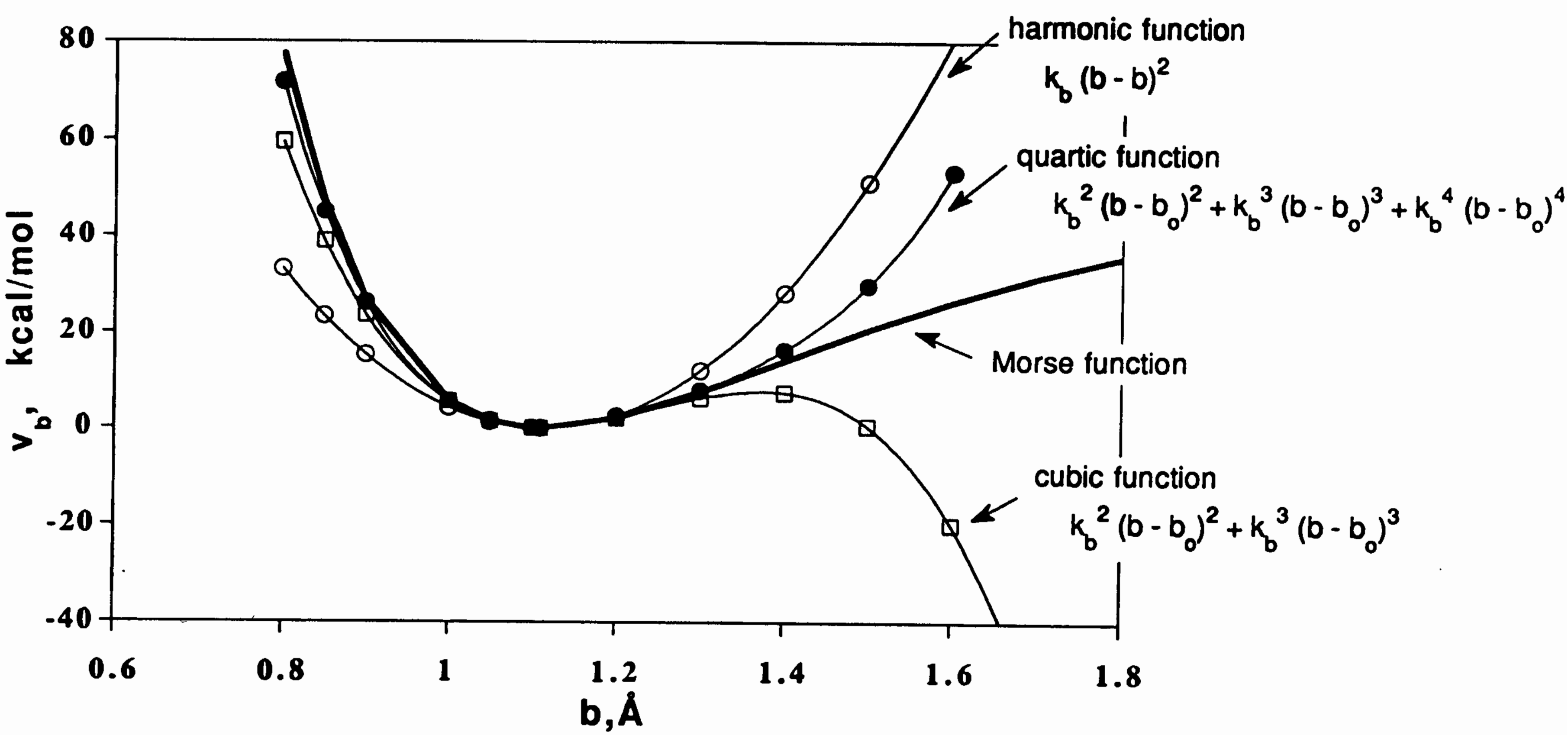

Figure 3 Schematic of a Morse function and the related harmonic, cubic, and quartic potentials (Eqs. [3] and [4]). When the bond length is increased beyond the point of the minimum, the harmonic potential rises too steeply. The cubic term corrects for the anharmonicity locally, but at longer distances turns and goes catastrophically to negative infinity. The quartic potential remains a good approximation over a relatively large range and is always attractive at large distances.

ANGLE POTENTIALS

$$E(\theta) = \frac{1}{2} k \,(\theta - \theta_0)^2$$

$$E(R,\theta) = \frac{1}{2} k \,(R - R_0)(\theta - \theta_0)$$

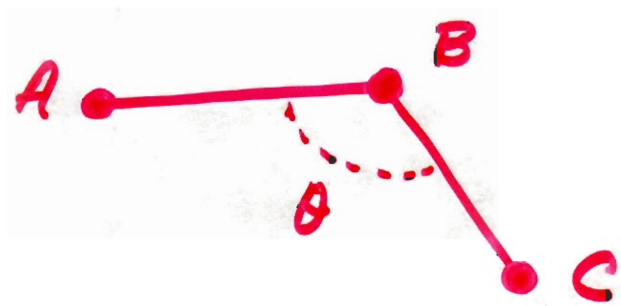

TORSIONAL POTENTIAL

$$E(\omega) = \sum_J \frac{1}{2} k_J \Big(1 - \cos(J \cdot \omega)\Big)$$

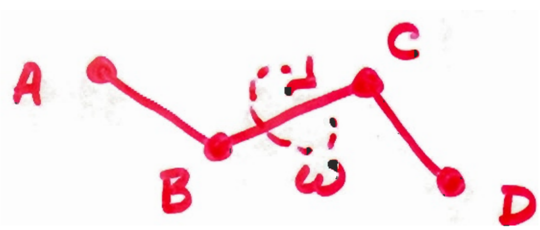

$\omega \approx -120°$

$$v(\omega) = \sum_{n=0}^{N} \frac{V_n}{2} [1 + \cos(n\omega - \gamma)]$$

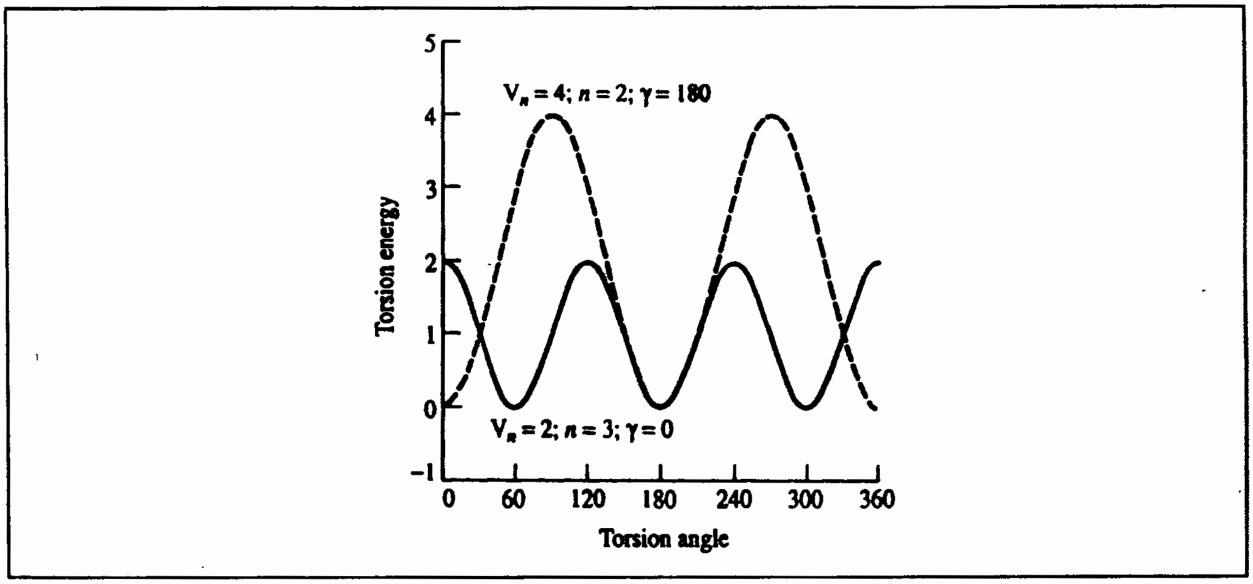

Fig. 4.7: Torsional potential varies as shown for different values of V_n, n and γ.

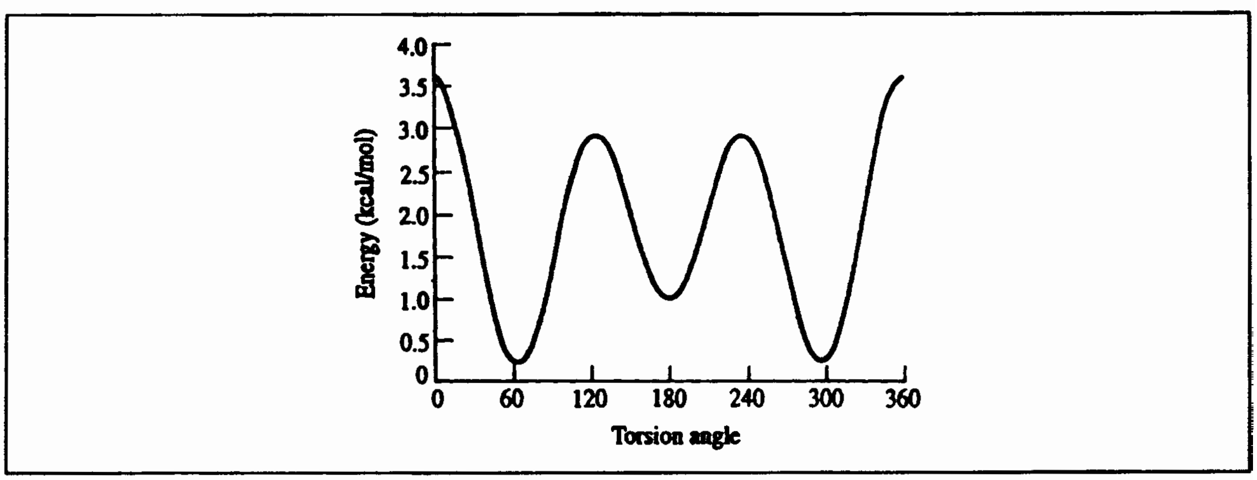

Fig. 4.8: Variation in torsional energy (AMBER force field) with O–C–C–O torsion angle (ω) for OCH_2-CH_2O fragment. The minimum energy conformations arise for $\omega = 60°$ and $300°$.

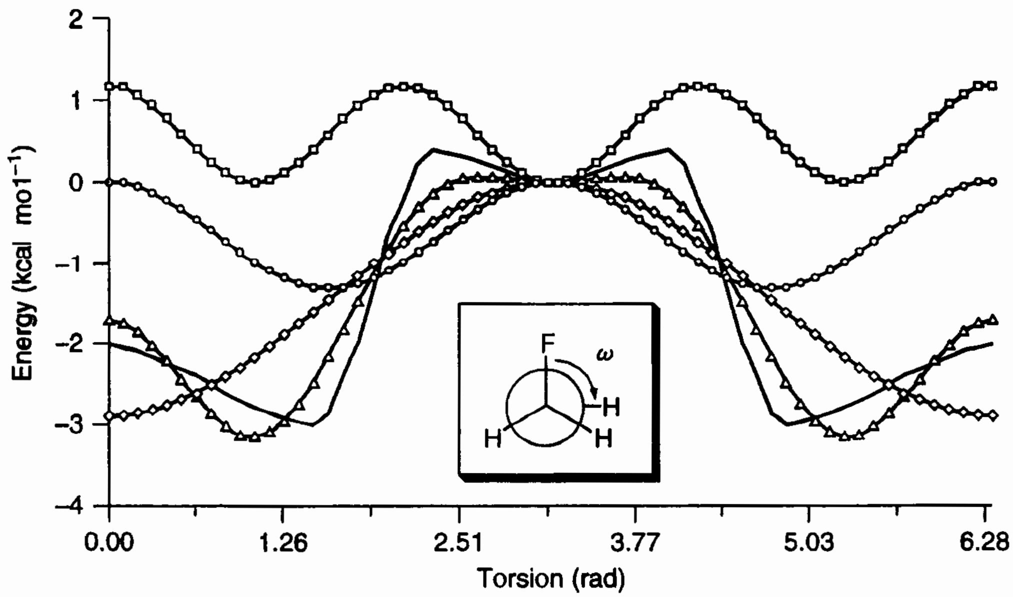

Figure 2.3 Fourier decomposition of the torsional energy for rotation about the C–O bond of fluoromethanol (bold black curve, energetics approximate). The Fourier sum (Δ) is composed of the onefold (◇), twofold (○), and threefold (□) periodic terms, respectively. In the Newman projection of the molecule, the oxygen atom lies behind the carbon atom at center

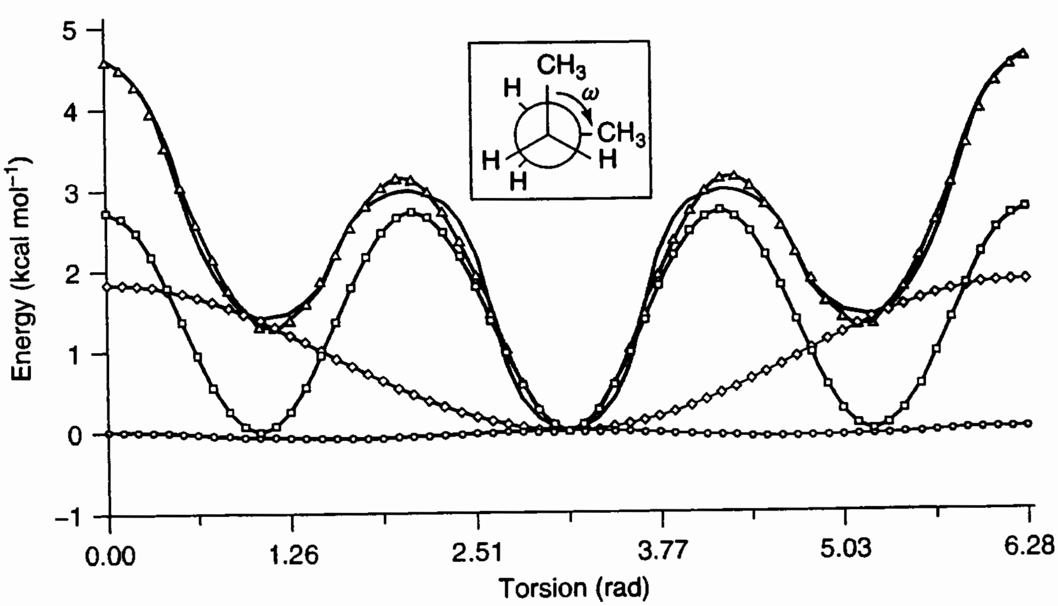

Figure 2.4 Fourier decomposition of the torsional energy for rotation about the C–C bond of *n*-butane (bold black curve, energetics approximate). The Fourier sum (Δ) has a close overlap, and is composed of the onefold (◇), twofold (○), and threefold (□) periodic terms, respectively

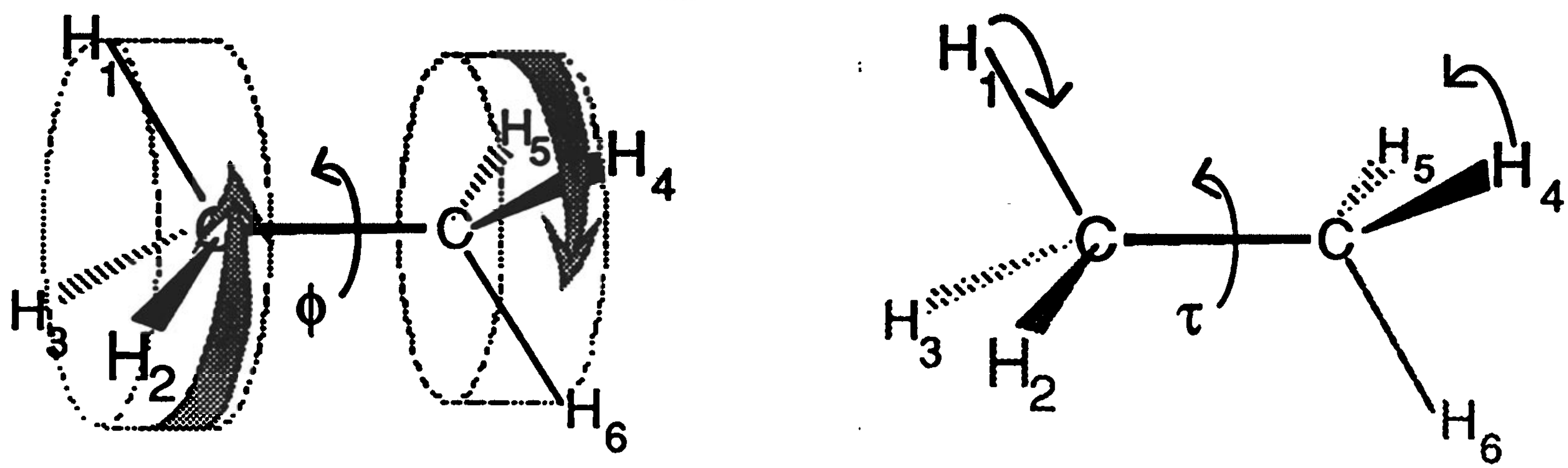

Figure 4 Rigid internal rotation (torsional angle ϕ) involving the methyl group as a unit, and the dihedral motions (τ), which describe a single H—C—C—H deformation, in ethane. Although there is a single definition of ϕ, there are 9 independent choices for τ.

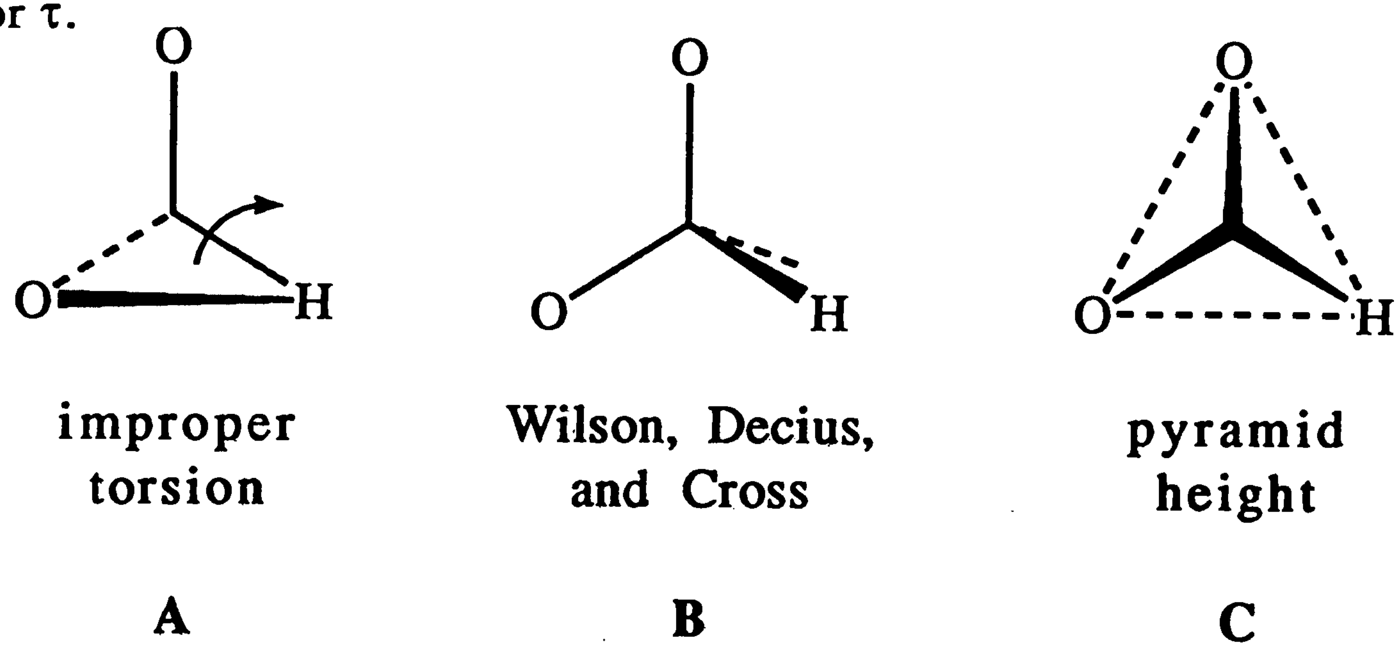

Figure 5 Definitions of out-of-plane coordinate. The molecule shown is the formate anion. The improper torsion definition is nonphysical and is used only because it can be easily adapted to existing torsional models and programs.

OUT-OF-PLANE-BEND:

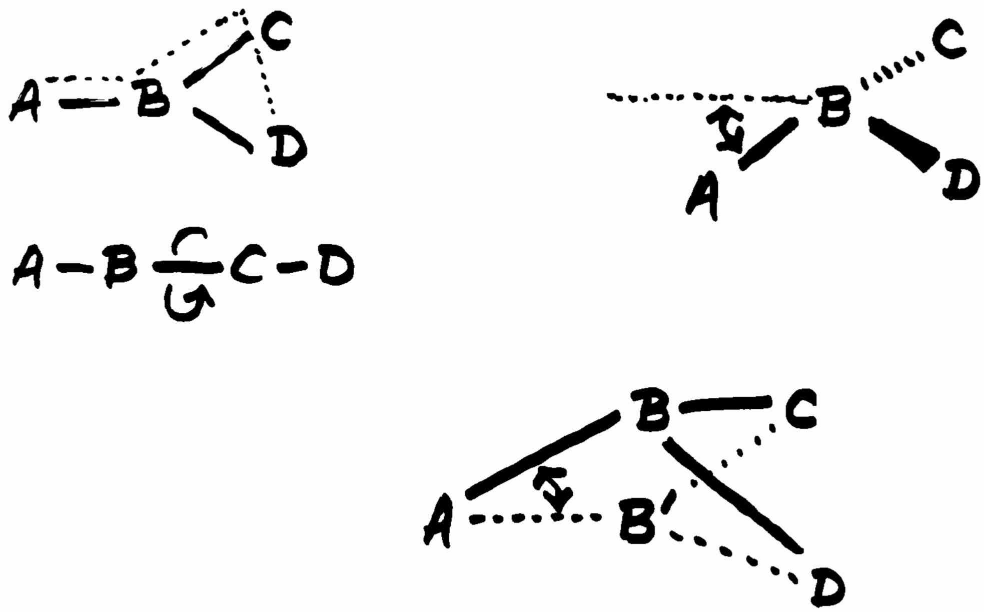

HYDROGEN ATOM OFFSET:

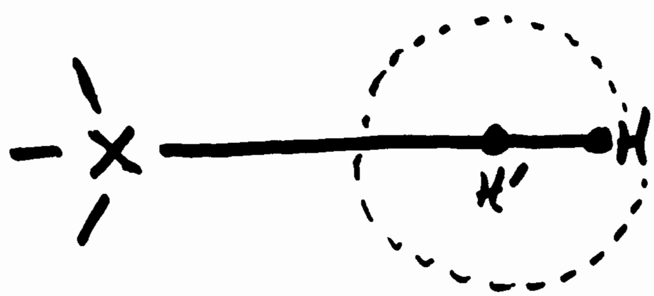

C–H .92
N–H .8

OFF-CENTER BOND DIPOLES:

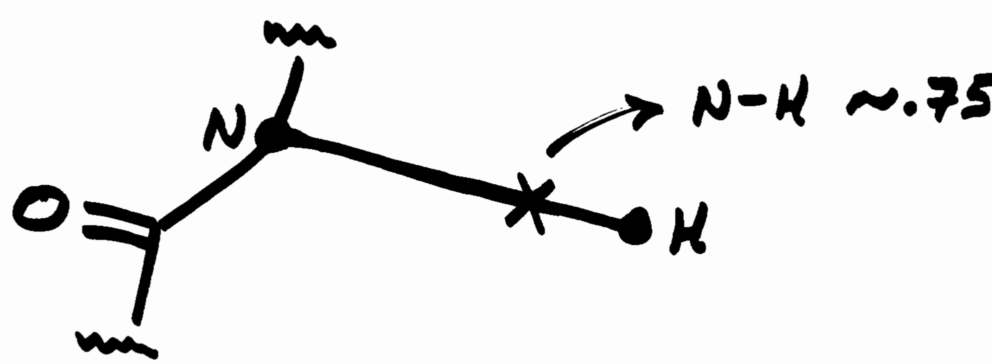

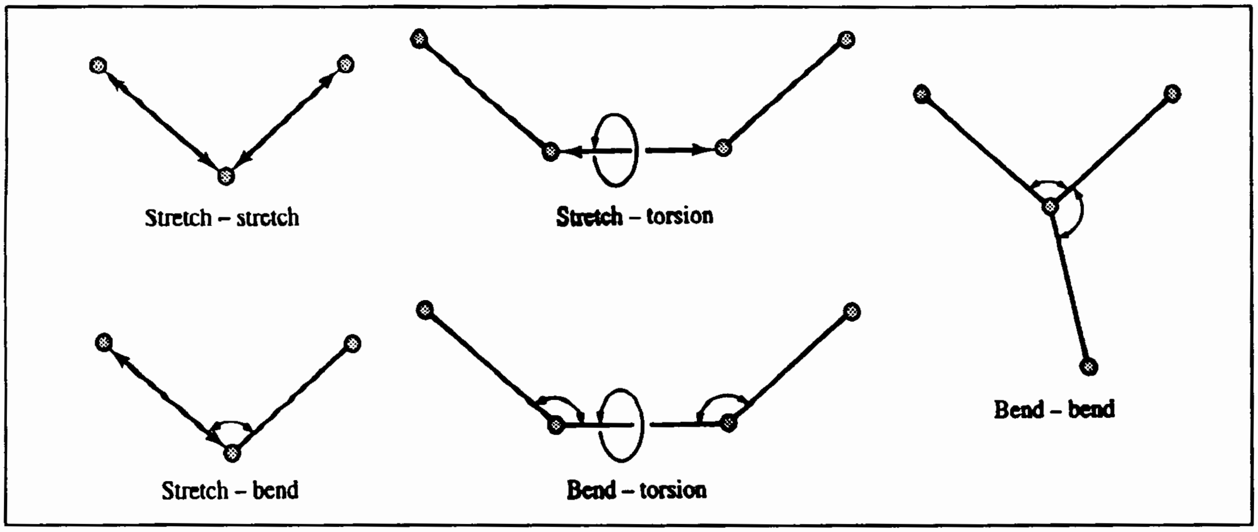

Fig. 4.13: Schematic illustration of the cross terms believed to be most important in force fields. (Adapted from Dinur U and A T Hagler 1991. New Approaches to Empirical Force Fields. In Reviews in Computational Chemistry, *Lipkowitz K B and D B Boyd (Editors). New York, VCH Publishers, pp. 99–164.)*

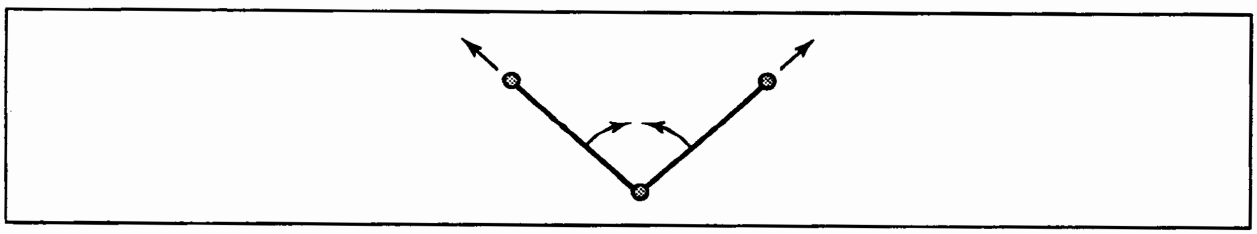

Fig. 4.12: Coupling between the stretching of the bonds as an angle closes.

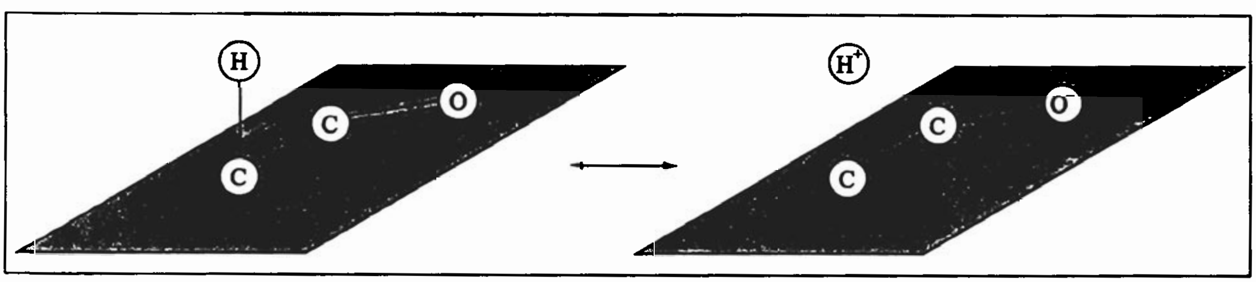

Fig. 4.14: Valence bond representation of the hyperconjugation effect which leads to a lengthening of the C–H bond in acetaldeyde.

VAN der WAALS POTENTIAL

LENNARD - JONES

$$E(R) = \varepsilon \left\{ \left(R_o/R\right)^{12} - \left(R_o/R\right)^{6} \cdot 2 \right\}$$

BUCKINGHAM

$$E(R) = 2.9 \cdot 10^{5}\, \varepsilon\, e^{-12.5 (R_o/R)} - 2.25\, \varepsilon \left(R_o/R\right)^{6}$$

PROBLEM –

MANY BODY EFFECTS SUCH AS POLARIZABILITY AND SHIELDING

ANISOTROPY, ESPECIALLY FOR HYDROGENS

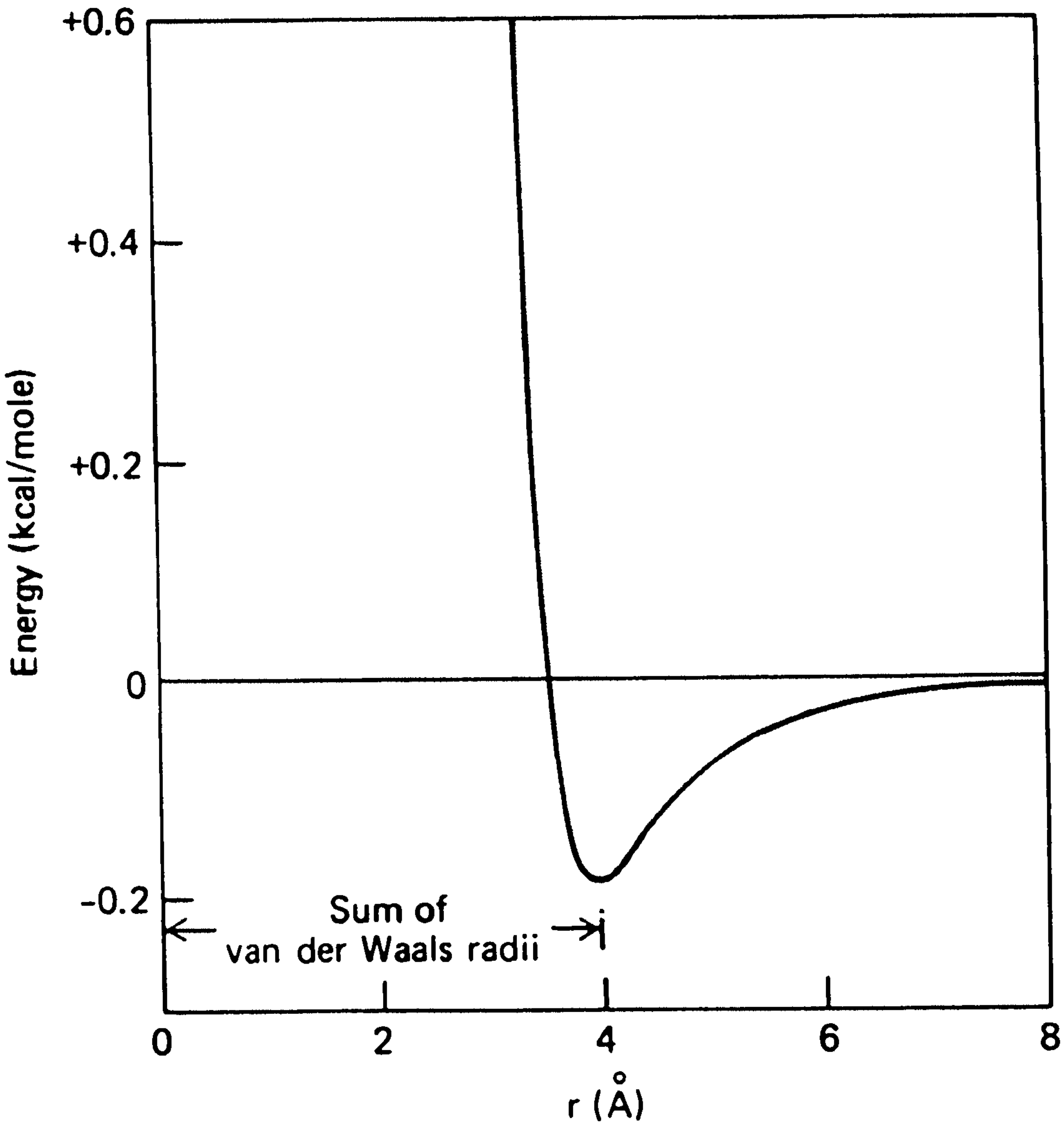
+0.6
+0.4
+0.2
0
-0.2
Energy (kcal/mole)
Sum of
van der Waals radii
0
2
4
6
8
r (Å)

A

B

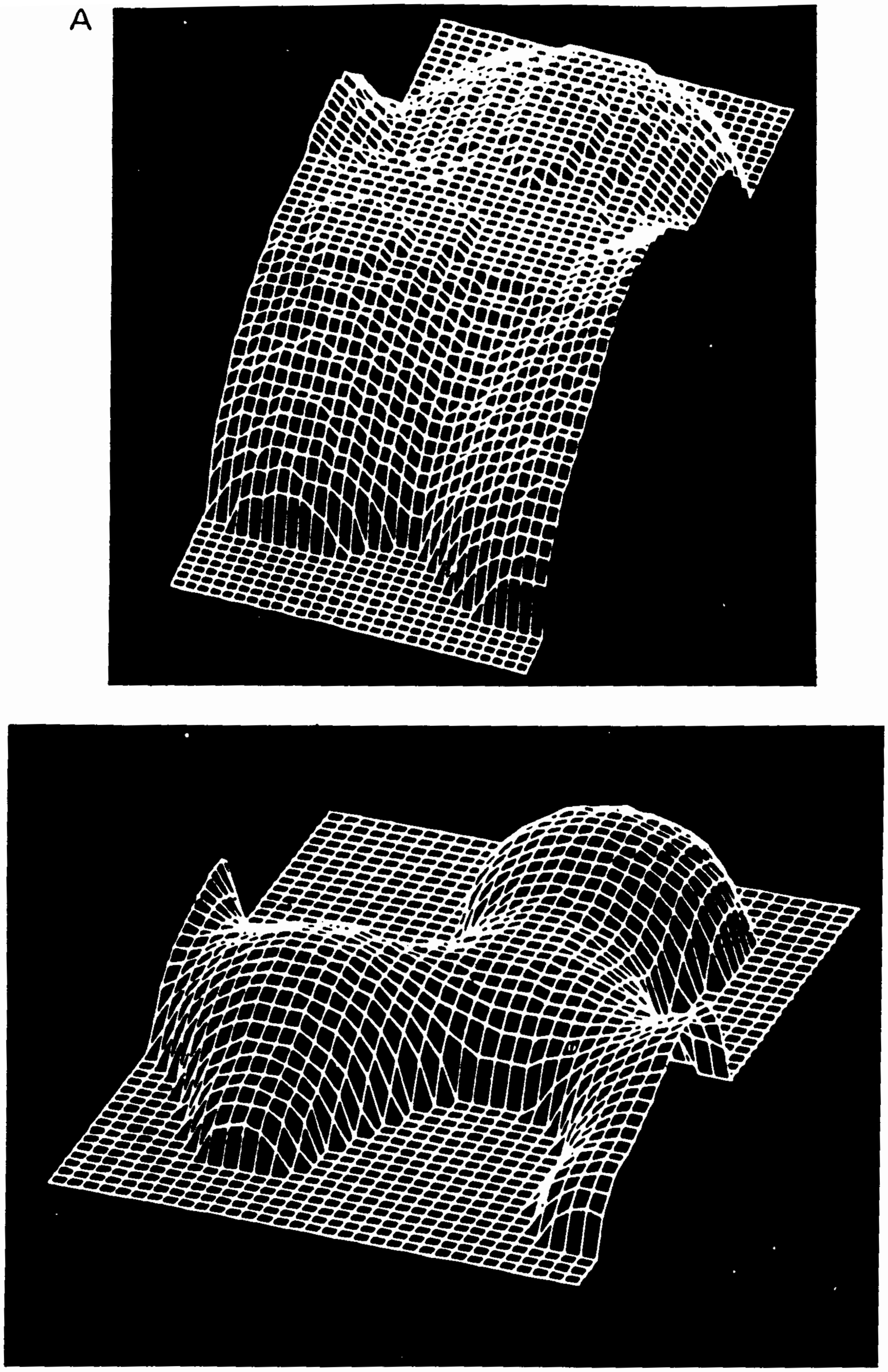

Fig. 1. The overall three-dimensional shape of the amide group in AcNHMe. The carbonyl group is on the right with the oxygen at the top of the figure, while the N-H is trans-directed toward the lower border of the plane. (A) Surface of constant electron density of 0.027 electrons/Å^3, roughly corresponding to van der Waals radius. (B) Surface of constant electron density of 0.75 electron/Å^3.

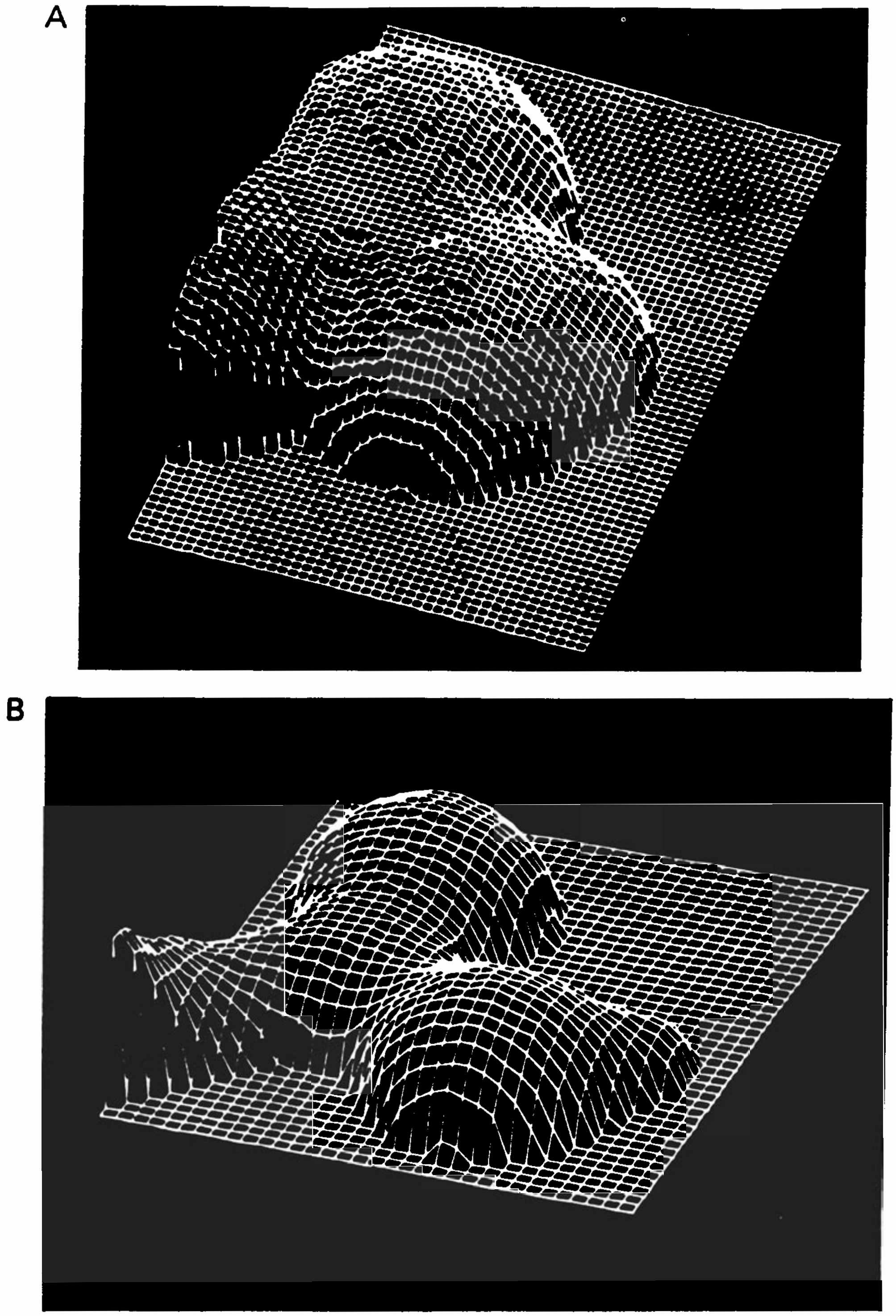

Fig. 2 The overall three-dimensional shape of the carboxyl group in acetic acid. The carboxyl group is on the left with the oxygen at the top of the figure, while the O-H is cis and in the foreground directed to the right. (A) Surface of constant electron density of 0.027 electrons/Å^3, roughly corresponding to van der Waals radius. (B) Surface of constant electron density of 0.75 electrons/Å^3.

Types of VDW Potentials

Exponential

$$Ae^{-Br} - Cr^{-6}$$

Lennard-Jones

$$\varepsilon\{(r_m/r)^n - 2(r_m/r)^6\}$$

Maitland-Smith

$$\varepsilon\{(6/n-6)(r_m/r)^n - (n/n-6)(r_m/r)^6\}$$

with $n = 13 - \gamma(r/r_m) - \gamma$

R^{-6} POLARIZATION TERM

$$E = E_{ELEC} + E_{IND} + E_{DISP}$$

$$E = -\frac{1}{(4\pi\varepsilon_0)^2}\left\{\underbrace{\frac{2}{3}\frac{\mu^4}{kT}}_{\text{ELEC}} + \underbrace{2\mu^2\alpha}_{\text{IND}} + \underbrace{\frac{3}{4}\alpha^2\hbar\omega_0}_{\text{DISP}}\right\}R^{-6}$$

	ELEC	IND	DISP
Ar	0	0	50
CO	.003	.06	97
NH_3	64	9	133
H_2O	184	10	61

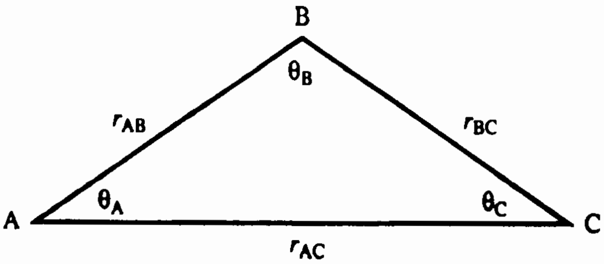

Fig. 4.37: Calculating the three-body Axilrod–Teller contribution.

Three-body effects can significantly affect the dispersion interaction. For example, it is believed that three-body interactions account for approximately 10% of the lattice energy of crystalline argon. For very precise work, interactions involving more than three atoms may have to be taken into account, but they are usually small enough to be ignored. A potential that includes both two- and three-body interactions would be written in the following general form:

$$\mathscr{V}(\mathbf{r}^N) = \sum_{i=1}^{N} \sum_{j=i+1}^{N} v^{(2)}(r_{ij}) + \sum_{i=1}^{N} \sum_{j=i+1}^{N} \sum_{k=j+1}^{N} v^{(3)}(r_{ij}, r_{ik}, r_{jk}) \tag{4.80}$$

Axilrod and Teller investigated the three-body dispersion contribution and showed that the leading term is:

$$v^{(3)}(r_{AB}, r_{AB}, r_{BC}) = \nu_{A,B,C} \frac{3\cos\theta_A \cos\theta_B \cos\theta_C}{(r_{AB} r_{AC} r_{BC})^3} \tag{4.81}$$

θ_A, θ_B and θ_C are the internal angles of the triangle with sides of length r_{AB}, r_{AC} and r_{BC} (Figure 4.37). $\nu_{A,B,C}$ is a constant characteristic of the three species A, B and C. If A, B and C are identical then $\nu_{A,B,C}$ is approximately related to the Lennard-Jones coefficient C_6 and the polarisability by

$$\nu_{A,B,C} = -\frac{3\alpha C_6}{4(4\pi\varepsilon_0)} \tag{4.82}$$

The effect of the Axilrod–Teller term (also known as the triple-dipole correction) is to make the interaction energy more negative when three molecules are linear but to weaken it when the molecules form an equilateral triangle. This is because the linear arrangement enhances the correlations of the motions of the electrons, whereas the equilateral arrangement reduces it.

The three-body contribution may also be modelled using a term of the form $v^{(3)}(r_{AB}, r_{AC}, r_{BC}) = K_{A,B,C}\{\exp(-\alpha r_{AB})\exp(-\beta r_{AC})\exp(-\gamma r_{BC})\}$ where K, α, β and γ are constants describing the interaction between the atoms A, B and C. Such a functional form has been used in simulations of ion–water systems, where polarisation alone does not exactly model configurations when there are two water molecules close to an ion [Lybrand and Kollman 1985]. The three-body exchange repulsion term is thus only calculated for ion–water–water trimers when the species are close together.

ELECTROSTATIC POTENTIALS

CHARGE-CHARGE

$$E(R) = 332\, q_1 q_2 / DR$$

DIPOLE-DIPOLE

$$E(\mu_1, \mu_2) = (\cos\kappa - 3\cos\alpha \cos\beta) \cdot \mu_1 \mu_2 / DR^3$$

(JEANS' FORMULA)

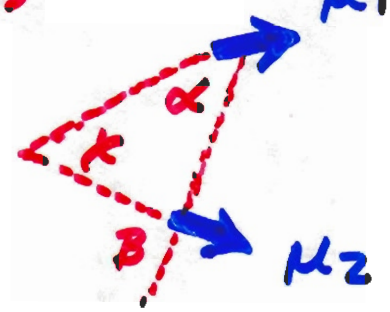

SIMILARLY, CHARGE-DIPOLE $\propto 1/R^2$

PROBLEMS — VALUE OF D ?
H-BONDING POTENTIALS ?

Partial Atomic Charges for Serine Residues

ATOM	CHARMM 19	CHARMM 22	AMBER 84	AMBER 95	OPLS UA	OPLS AA	BUFF	GROMOS 96
N	-0.35	-0.47	-0.463	-0.416	-0.57	-0.50	-0.749	-0.28
HN	0.25	0.31	0.252	0.272	0.37	0.30	0.328	0.28
CA	0.10	0.07	0.035	-0.025	0.20	0.14	0.189	0.00
HA	–	0.09	0.048	0.084	–	0.06	0.048	–
C	0.55	0.51	0.616	0.597	0.50	0.50	0.828	0.38
O	-0.55	-0.51	-0.504	-0.568	-0.50	-0.50	-0.679	-0.38
CB	0.25	0.05	0.018	0.212	0.265	0.145	0.296	0.15
HB	–	0.09	0.119	0.035	–	0.06	0.006	–
OG	-0.65	-0.66	-0.55	-0.655	-0.70	-0.683	-0.764	-0.548
HO	0.40	0.43	-0.31	0.428	0.435	0.418	0.491	0.398

4.9.2 Point-charge Electrostatic Models

We therefore return to the point-charge model for calculating electrostatic interactions. If sufficient point charges are used then all of the electric moments can be reproduced and the multipole interaction energy, Equation (4.30), is exactly equal to that calculated from the Coulomb summation, Equation (4.19).

An accurate representation of a molecule's electrostatic properties may require charges to be placed at locations other than at the atomic nuclei. A simple example of this is molecular nitrogen, which has a dipole moment of zero. The total charge on nitrogen is zero, and so an atomic partial charge model would put zero charge on each nucleus. However, nitrogen does have a quadrupole moment and this significantly affects its properties. The simplest way to model this is to place three partial charges along the bond: a charge of $-q$ at each nucleus and $+2q$ at the centre of mass. The quadrupole–quadrupole interaction between two nitrogen molecules can then be calculated by summing nine pairs of charge–charge interactions. The value of q can be calculated using the following relationship between the quadrupole moment and the partial charge:

$$\Theta = 2q(l/2)^2 \tag{4.31}$$

l is the bond length. The experimental quadrupole moment is consistent with a charge, q, of approximately 0.5e. In fact, a better representation of the electrostatic potential around the nitrogen molecule is obtained using the five-charge model shown in Figure 4.20.

An alternative to the point charge model is to assign dipoles to the bonds in the molecule. The electrostatic energy is then given as a sum of dipole–dipole interaction energies. This approach (which is adopted in MM2/MM3/MM4) can be unwieldy for molecules that have a formal charge and which require charge–charge and charge–dipole terms to be included in the energy expression. Charged species are dealt with more naturally using the point charge model.

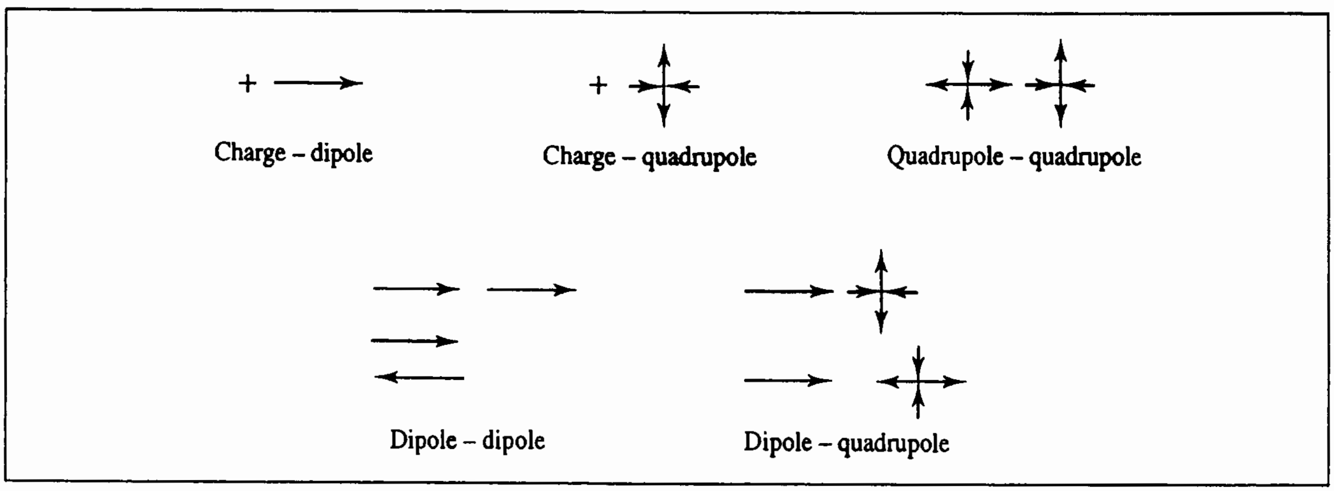

Fig. 4.18: The most favourable orientations of various multipoles. (Figure adapted from Buckingham A D 1959. Molecular Quadrupole Moments. Quarterly Reviews of the Chemical Society *13:183–214.)*

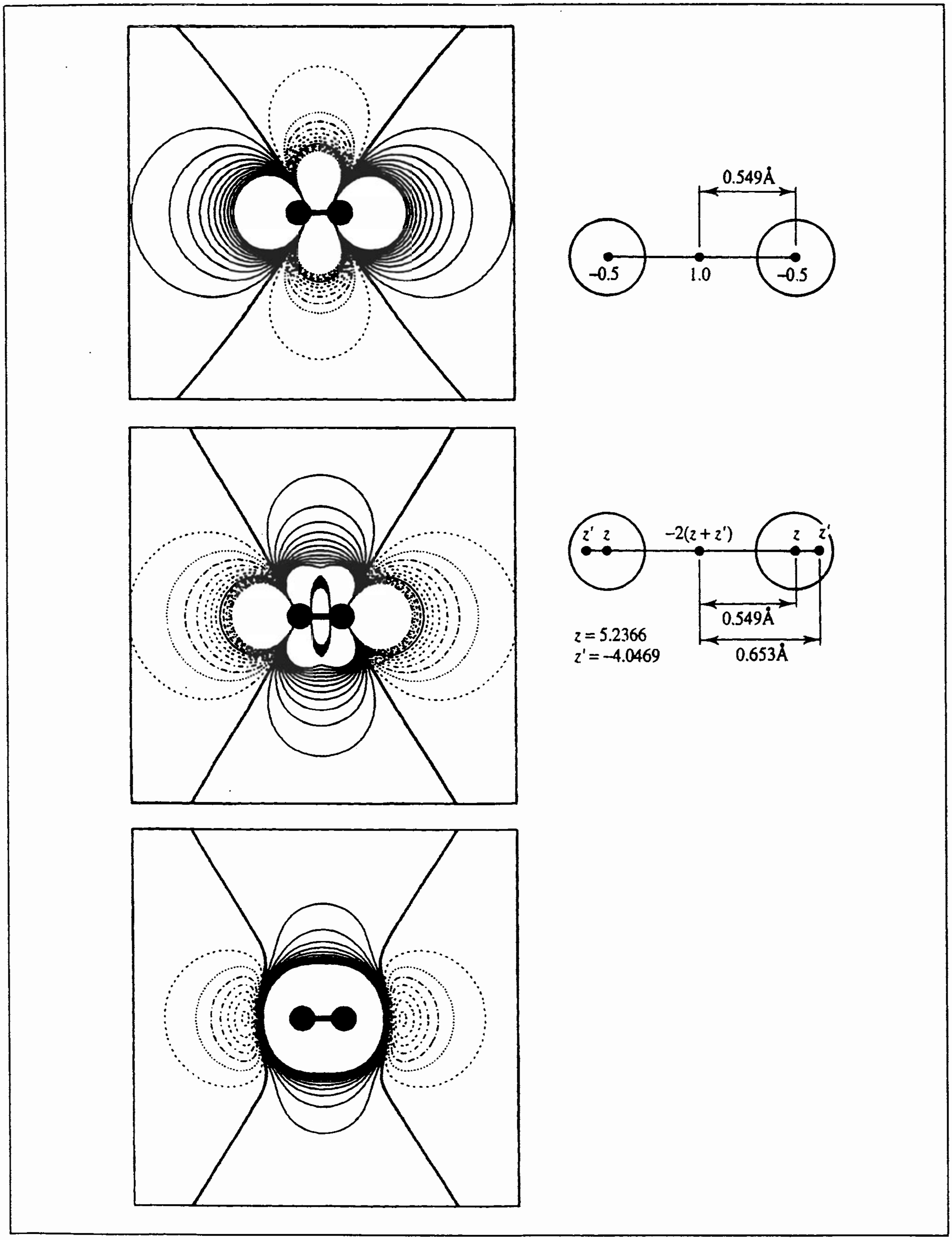

Fig. 4.20: Two charge models for N_2 with the electrostatic potentials that they generate. Also shown is the electrostatic potential calculated using ab initio *quantum mechanics (6-31G* basis set.) Negative contours are dashed and the zero contour is bold.*

Table 12 Goodness-of-Fit of PD Atomic Multipole Expansions and Bond Dipole Models[a]

Molecule	M	M + D	M + D + Q	D	BD	RBD
Methane	0.21	0.02	0.01	0.11	0.32	0.32
	13.53	1.04	0.39	6.88	20.05	20.05
Ethylene	1.19	0.20	0.02	0.58	0.30	1.12
	15.93	2.66	0.21	7.73	3.99	14.91
Acetylene	0.19	0.01	0.00	0.02	0.35	0.35
	1.34	0.06	0.02	0.14	2.46	2.46
Hydrogen fluoride	2.20	0.13	0.00	1.25	2.20	2.24
	7.54	0.41	0.00	4.28	7.53	7.65
Methyl fluoride	1.01	0.18	0.01	0.61	0.90	1.15
	4.38	0.78	0.03	2.63	3.45	5.03
Water	2.67	0.22	0.00	2.14	1.37	2.74
	8.44	0.88	0.01	6.76	4.35	8.73
Methanol	1.98	0.31	0.00	0.78	0.62	1.77
	8.35	1.31	0.02	3.29	2.60	7.33
Dimethyl ether	1.72	0.25	0.00	0.27	0.71	1.82
	9.49	1.37	0.02	1.47	3.93	9.82
Carbon dioxide	0.65	0.02	0.00	1.55	0.21	0.21
	5.08	0.12	0.00	12.09	1.65	1.65
Formaldehyde	1.22	0.59	0.03	1.66	1.10	1.14
	3.84	1.86	0.11	5.21	3.48	3.63
Acetaldehyde	1.19	0.38	0.02	0.78	0.63	1.15
	3.90	1.23	0.05	2.55	2.05	3.81
Acetone	0.70	0.30	0.01	0.65	0.48	0.55
	2.31	0.98	0.02	2.14	1.58	1.85
Formic acid	1.80	0.38	0.02	1.20	0.72	1.61
	6.64	1.28	0.07	4.45	2.66	6.05
Acetic acid	0.89	0.23	0.01	0.86	0.43	1.01
	3.65	0.94	0.03	3.54	1.76	4.16
Methyl formate	2.11	0.23	0.01	0.92	0.62	1.75
	9.21	1.00	0.04	4.02	2.70	7.59
Methyl acetate	1.28	0.14	0.00	0.64	0.48	0.92
	6.03	0.67	0.02	3.03	2.28	4.25
Ammonia	2.66	0.62	0.01	1.20	0.63	2.41
	9.90	2.31	0.02	4.45	2.36	9.20
Methyl amine	2.79	0.38	0.00	0.57	0.71	2.47
	13.74	1.87	0.02	2.78	3.50	12.68
Dimethyl amine	2.66	0.24	0.01	0.39	0.74	2.57
	16.27	1.48	0.03	2.38	3.50	16.87
Trimethyl amine	1.36	0.15	0.01	0.30	0.64	1.23
	11.68	1.25	0.05	2.58	5.53	11.40
Formamide	1.65	0.29	0.01	0.91	0.56	1.59
	3.68	0.65	0.03	2.03	1.24	3.53
Acetamide	0.67	0.21	0.00	0.67	0.33	0.50
	1.69	0.52	0.01	1.67	0.82	1.24
N-Methylformamide	1.63	0.18	0.01	0.58	0.45	1.65
	4.20	0.46	0.02	1.49	1.16	4.24
N-Methylacetamide	1.11	0.10	0.00	0.86	0.45	1.05
	3.26	0.30	0.01	2.44	1.28	2.86

[a]The first row gives rms in kJ/mol; the second rrms in %.

	SPC	SPC/E	TIP3P	BF	TIP4P	ST2
r(OH), Å	1.0	1.0	0.9572	0.96	0.9572	1.0
HOH, deg	109.47	109.47	104.52	105.7	104.52	109.47
$A \times 10^{-3}$, kcal Å^{12}/mol	629.4	629.4	582.0	560.4	600.0	238.7
C, kcal Å^{6}/mol	625.5	625.5	595.0	837.0	610.0	268.9
q(O)	−0.82	−0.8472	−0.834	0.0	0.0	0.0
q(H)	0.41	0.4238	0.417	0.49	0.52	0.2375
q(M)	0.0	0.0	0.0	−0.98	−1.04	−0.2375
r(OM), Å	0.0	0.0	0.0	0.15	0.15	0.8

Table 4.3 A comparison of various water models [Jorgensen et al. *1983]. For the ST2 potential, q(M) is the charge on the 'lone pairs', which are a distance 0.8 Å from the oxygen atom (see Figure 4.40).*

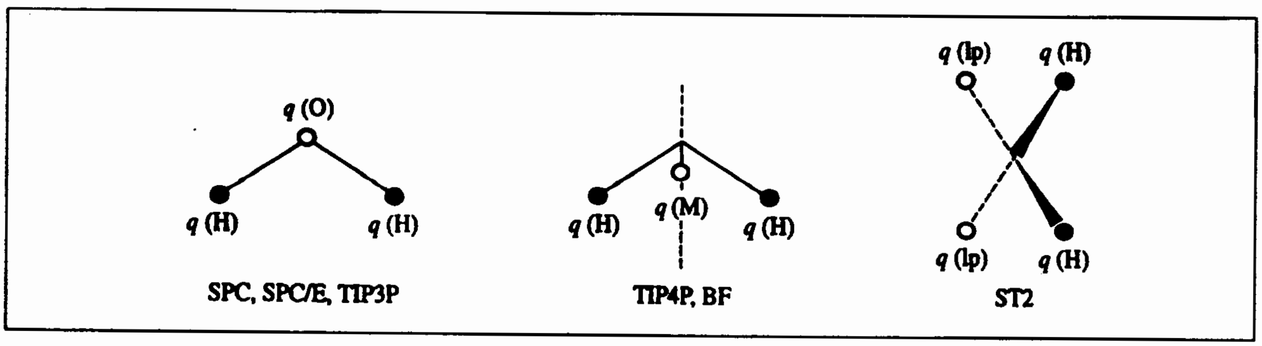

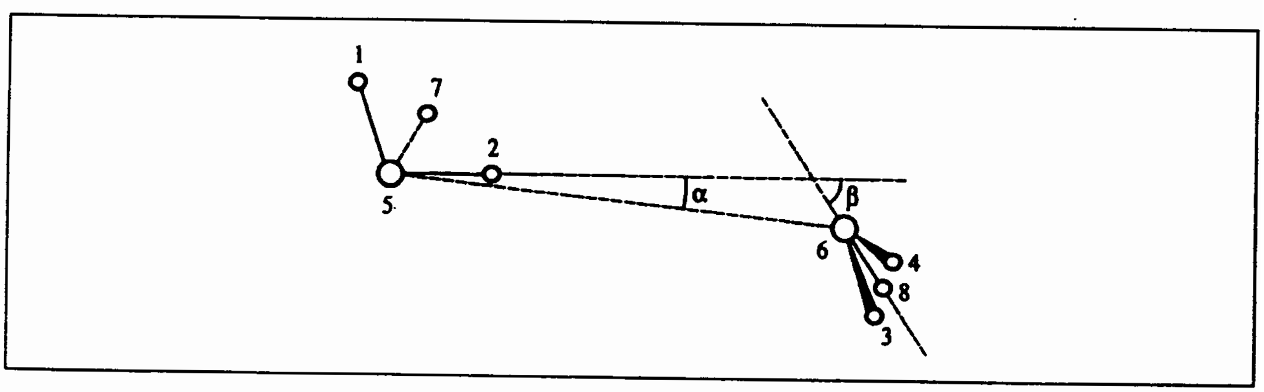

SIMULATING LIQUID WATER

- Very simple model
  - 3 interaction centers
  - Completely flexible
  - Smooth cutoff at 6 Å (list to 8Å)

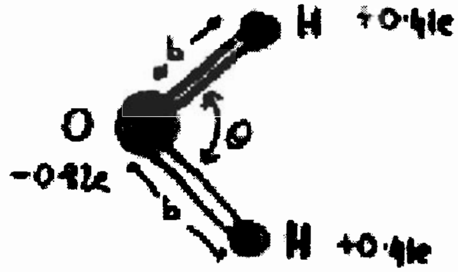

Electrostatics } long range forces
Van der Waals

- Good fit to experiment

Property	Experiment (25 °c)	Simulation
Potential energy (kcal/mol)	-9.2	-9.5
Pressure (atmospheres)	1	-61
Classical Specific Heat (cal/°K)	27	26
Diffusion Constant ($Å^2$/ps)	0.23	0.22
Rotational Relaxation Time (ps)	2	1.6
Radial Distribution Function r_1	2.8	2.7
h_1	$\boxed{\cancel{2.5}}$ 3.0*	$\boxed{3.2}$
r_2	3.3	3.3
h_2	0.8	0.8
r_3	4.6	4.3
h_3	1.11	1.09

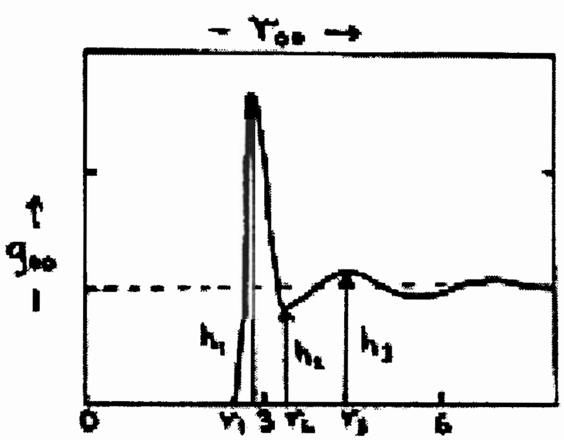

* Calibration error fixed after 15 years of experiment

Derivatives of the Molecular Mechanics Energy Function

Many molecular modelling techniques that use force-field models require the derivatives of the energy (i.e. the force) to be calculated with respect to the coordinates. It is preferable that analytical expressions for these derivatives are available because they are more accurate and faster than numerical derivatives. A molecular mechanics energy is usually expressed in terms of a combination of internal coordinates of the system (bonds, angles, torsions, etc.) and interatomic distances (for the non-bonded interactions). The atomic positions in molecular mechanics are invariably expressed in terms of Cartesian coordinates (unlike quantum mechanics, where internal coordinates are often used). The calculation of derivatives with respect to the atomic coordinates usually requires the chain rule to be applied. For example, for an energy function that depends upon the separation between two atoms (such as the Lennard-Jones potential, Coulomb electrostatic interaction or bond-stretching term) we can write:

$$r_{ij} = \sqrt{(x_i - x_j)^2 + (y_i - y_j)^2 + (z_i - z_j)^2} \tag{4.96}$$

$$\frac{\partial \mathcal{v}}{\partial x_i} = \frac{\partial \mathcal{v}}{\partial r_{ij}} \frac{\partial r_{ij}}{\partial x_i} \tag{4.97}$$

$$\frac{\partial r_{ij}}{\partial x_i} = \frac{(x_i - x_j)}{r_{ij}} \tag{4.98}$$

Thus, for the Lennard-Jones potential:

$$\frac{\partial \mathcal{v}}{\partial r_{ij}} = \frac{24\varepsilon}{r_{ij}} \left[-2\left(\frac{\sigma}{r_{ij}}\right)^{12} + \left(\frac{\sigma}{r_{ij}}\right)^{6} \right] \tag{4.99}$$

The force in the x direction acting on atom i due to its interaction with atom j is given by:

$$\mathbf{f}_{x_i} = (\mathbf{x}_i - \mathbf{x}_j) \frac{24\varepsilon}{r_{ij}^2} \left[2\left(\frac{\sigma}{r_{ij}}\right)^{12} - \left(\frac{\sigma}{r_{ij}}\right)^{6} \right] \tag{4.100}$$

Analytical expressions for the derivatives of the other terms that are commonly found in force fields are also available [Niketic and Rasmussen 1977]. Similar expressions must be derived from scratch when new functional forms are developed.

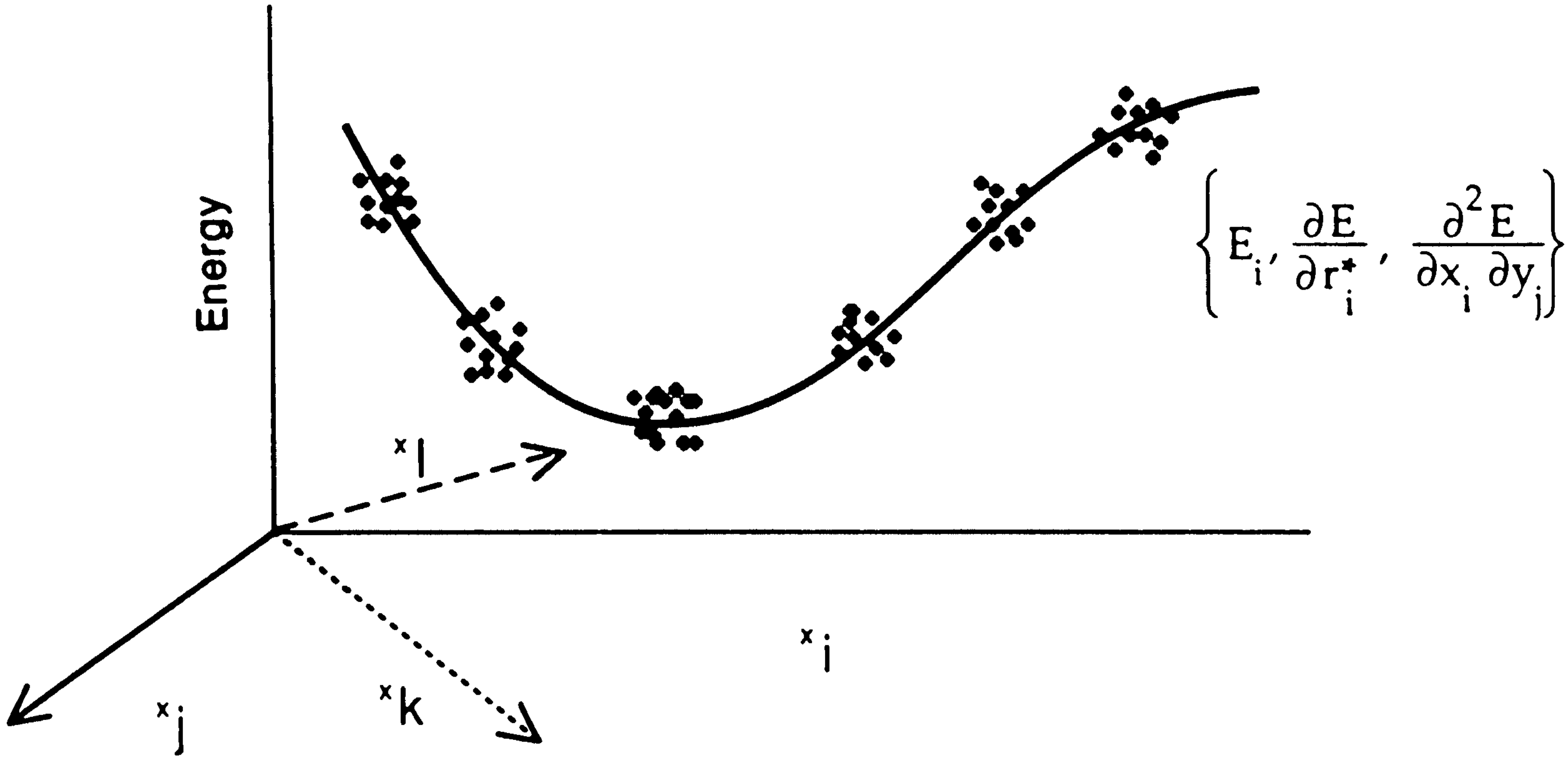

Figure 8 Sampling of a potential energy surface for formamide. The curve represents a potential energy profile. The cluster of points superimposed on the profile represents the multiple first and second derivatives of the energy for the configuration with that value on the *x*-coordinate. The number of data points for each configuration is one energy, *n* first derivatives, and $n(n + 1)/2$ second derivatives. This shows schematically that whereas a mapping of the energy from *ab initio* gives a single piece of information for each configuration *x*, the energy and first and second derivatives give far more information about the energy surface. In formamide, with only 6 atoms, each configuration yields only one energy, but there are 12 first derivatives and 78 second derivatives. Thus one obtains almost two orders of magnitude more information about the energy surface by using the gradient and second derivatives.

Vibrational Analysis:

Normal Modes

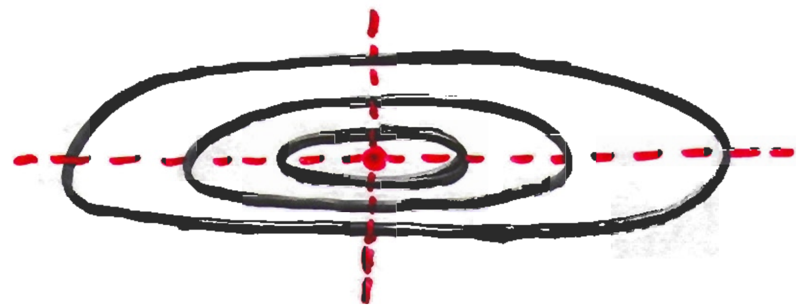

How Do We Get Them?

Diagonalize Mass Weighted Second Derivatives of the Potential Energy

Uses?

1. Compare w/ Expt. Frequencies
2. Estimate Conformational Entropy
3. Examine Low Frequency Motions of the Structure

LEVITT et al
JMB 181 423 (1985)

Figure 9. Showing the domain motion due to the lowest frequency modes in ribonuclease and lysozyme. The arrows on the α-carbon backbone are drawn as described in the legend to Fig. 8. (a) Ribonuclease, $\nu_1 = 2{\cdot}43\ \mathrm{cm}^{-1}$, period $= 13{\cdot}7$ ps. (b) Lysozyme, $\nu_1 = 2{\cdot}98\ \mathrm{cm}^{-1}$, period $= 11{\cdot}2$ ps.

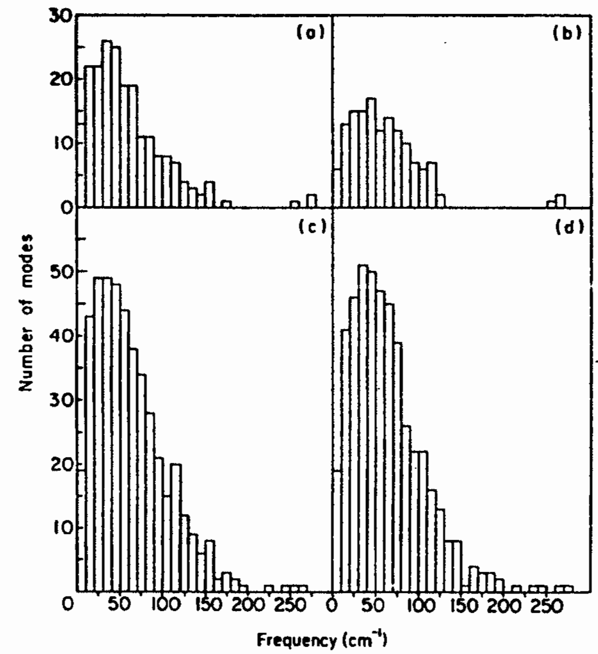

Figure 1. Showing the vibrational spectra calculated here with single-bond torsion angle variables. The number of modes with frequencies in a $10\ \mathrm{cm}^{-1}$ interval is plotted against frequency to give a density of states distribution. If each mode had the same intensity and a half line-width of $5\ \mathrm{cm}^{-1}$ the intensity envelope would be like the distribution shown. The spectra shown are for: (a) BPTI, (b) crambin, (c) ribonuclease and (d) lysozyme.

CONFORMATIONAL FREE ENERGY

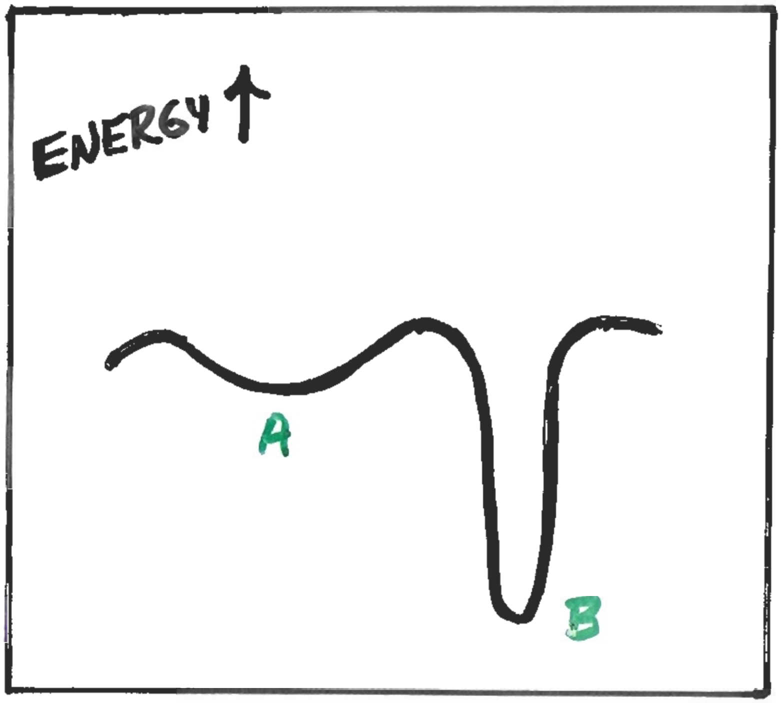

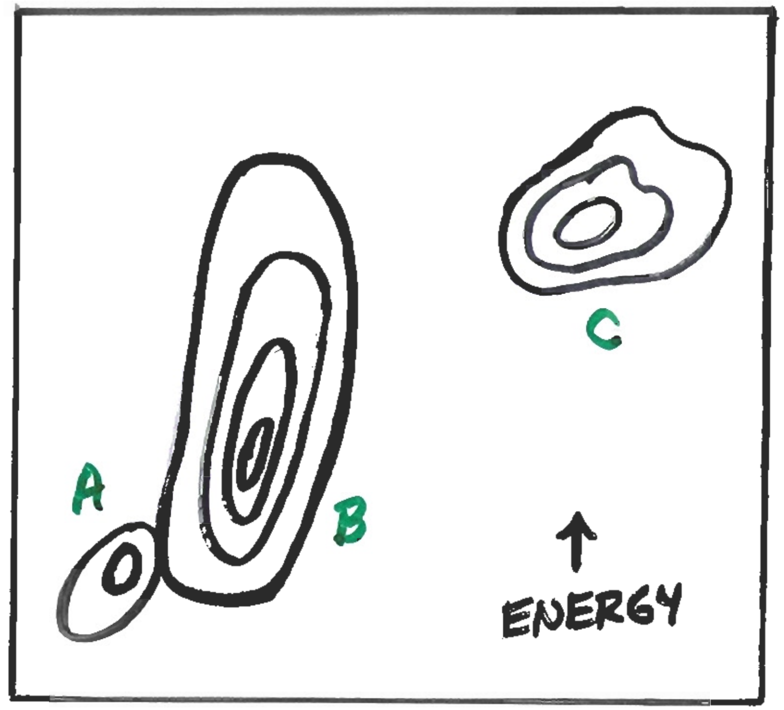

$$Z_{CONF} = \sum_{\tau_1, \tau_2} \exp\left[-E(\tau_1, \tau_2)/kT\right]$$

$$\Delta G^{\circ} = -kT \ln\left(Z_{CONF}\,A / Z_{CONF}\,B\right)$$